

Eastern North Pacific Hurricane Season of 2003

JOHN L. BEVEN II, LIXION A. AVILA, JAMES L. FRANKLIN, MILES B. LAWRENCE, RICHARD J. PASCH,
AND STACY R. STEWART

National Hurricane Center, Tropical Prediction Center, NOAA/NWS, Miami, Florida

(Manuscript received 13 April 2004, in final form 5 October 2004)

ABSTRACT

The tropical cyclone activity for 2003 in the eastern North Pacific hurricane basin is summarized. Activity during 2003 was slightly below normal. Sixteen tropical storms developed, seven of which became hurricanes. However, there were no major hurricanes in the basin for the first time since 1977. The first hurricane did not form until 24 August, the latest observed first hurricane at least since reliable satellite observations began in 1966. Five tropical cyclones made landfall on the Pacific coast of Mexico, resulting in 14 deaths.

1. Overview of the 2003 season

The National Hurricane Center (NHC) tracked 16 tropical cyclones (TCs) in the eastern North Pacific basin during 2003, all of which became tropical storms and 7 of which became hurricanes. This is at or slightly below the climatological average of 16 tropical storms and 9 hurricanes. However, no “major hurricanes” [category 3 or higher on the Saffir–Simpson hurricane scale (SSHS) (Simpson 1974)] with maximum 1-min average winds greater than 96 kt ($1 \text{ kt} = 0.514 \text{ m s}^{-1}$) formed during the season compared to the climatological average of four. This is the first time this has occurred in the basin since 1977, and examination of various meteorological parameters does not reveal a readily apparent explanation as to why.

Another interesting aspect to the season is that the first hurricane (Ignacio) did not form until 24 August. This is well past the climatological date of the first hurricane (17 June), and it is the latest first hurricane of record in the basin at least since 1966 when reliable satellite observations began.

Five cyclones made landfall on the Pacific coast of Mexico. Ignacio and Marty made landfall as hurricanes over the Baja California peninsula, causing 14 deaths. Carlos and Olaf came ashore as tropical storms in mainland Mexico, while Nora made landfall as a tropical depression in mainland Mexico. Jimena, which formed in the eastern North Pacific basin, threatened portions of the Hawaiian Islands.

As seen in past seasons, tropical waves play a significant to dominant role in TC development in the eastern

North Pacific Ocean. Avila et al. (2000) describe the methodology the NHC uses to track tropical waves from Africa across the tropical Atlantic, the Caribbean Sea, and Central America into the Pacific. Sixty-six tropical waves were tracked from the west coast of Africa across the tropical Atlantic and the Caribbean Sea from May to November 2003. Most of these waves reached the eastern North Pacific, where they played a role in tropical cyclogenesis, as noted in the individual cyclone summaries. It should be noted that midlatitude troughs interacting with the waves over the Atlantic during May and November made the count somewhat uncertain during those months. Thus, there could be a small error in the final wave total.

Figure 1 is a sequence of *Geostationary Operational Environmental Satellite-12 (GOES-12)* infrared images at 12-h intervals during 4–10 July 2003 showing the westward progression of a tropical wave across Central America into the Pacific. In the top image from 4 July, the wave and associated convective cluster are located over the southwestern Caribbean Sea. The sequence shows enhanced convection (marked by the dashed black line) propagating westward across Central America on 5 July and into the Pacific on 6 July. This convection subsequently becomes better organized on 9 July, and a tropical depression formed from it on 10 July. This later became Tropical Storm Enrique.

Section 2 describes the tropical storms and hurricanes of 2003 along with data sources used in analyzing and tracking them. Section 3 presents a discussion on the verification of NHC official forecasts.

2. Tropical storm and hurricane summaries

Individual cyclone summaries are based on “best track” data resulting from the NHC’s post-storm me-

Corresponding author address: Dr. John L. Beven II, National Hurricane Center, 11691 SW 17th St., Miami, FL 33165-2149.
E-mail: John.L.Beven@noaa.gov

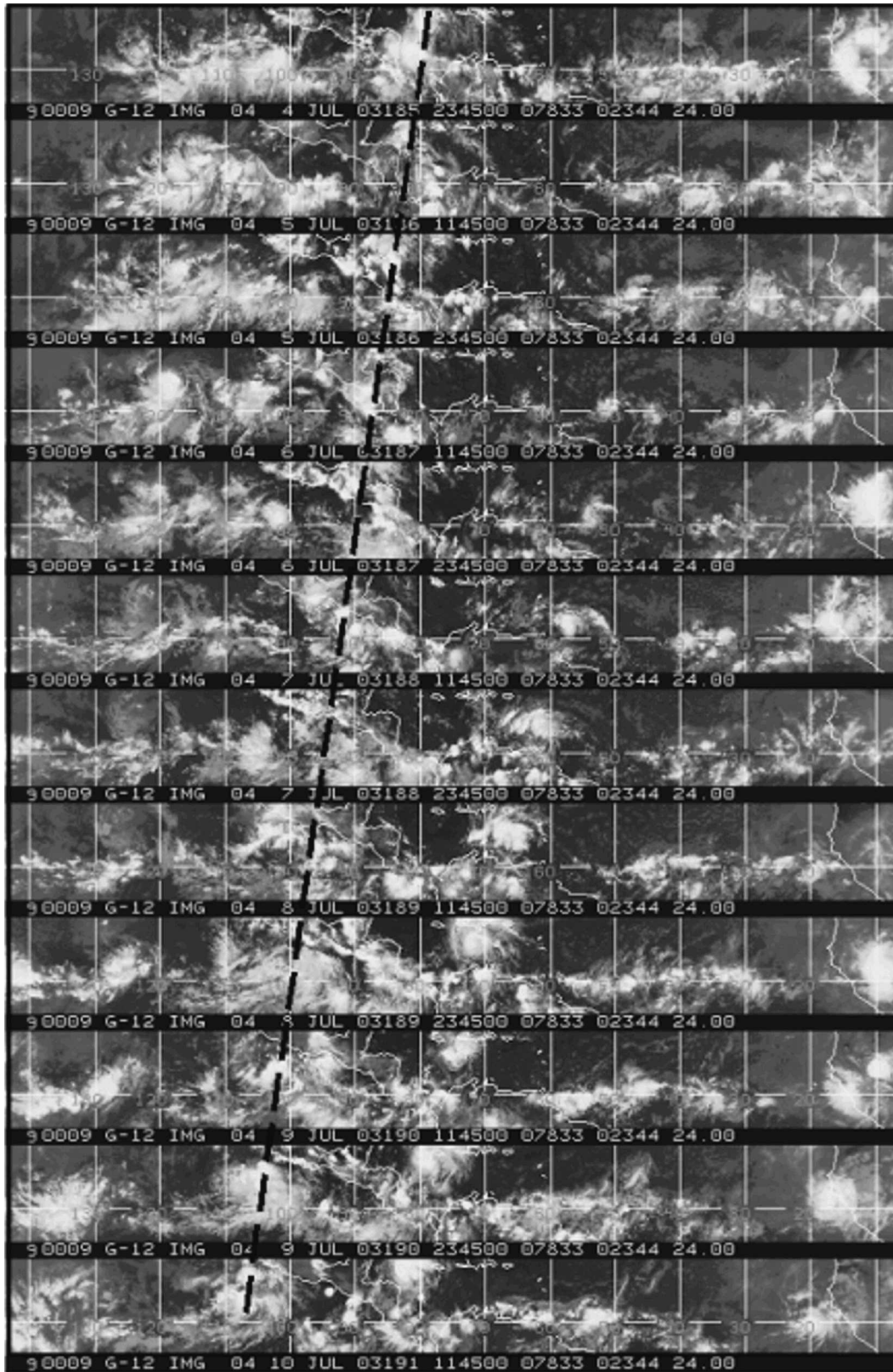


FIG. 1. Sequence of *GOES-12* infrared images at 12-h intervals from 4 to 10 Jul 2003. Dashed black line highlights the position of the tropical wave that developed into Tropical Storm Enrique on 10 Jul.

TABLE 1. Eastern North Pacific tropical storms and hurricanes of 2003.

Name	Class ^a	Dates ^b	Max 1-min wind speed (kt)	Min sea level pressure (mb)	Direct deaths
Andres	T	19–25 May	50	997	0
Blanca	T	17–22 Jun	50	997	0
Carlos	T	26–27 Jun	55	996	0
Dolores	T	6–8 Jul	35	1005	0
Enrique	T	10–15 Jul	55	993	0
Felicia	T	17–23 Jul	45	1000	0
Guillermo	T	7–12 Aug	50	997	0
Hilda	T	9–13 Aug	35	1004	0
Ignacio	H	22–27 Aug	90	970	2
Jimena ^c	H	28 Aug–5 Sep	90	970	0
Kevin	T	3–6 Sep	35	1000	0
Linda	H	13–17 Sep	65	987	0
Marty	H	18–24 Sep	85	970	12
Nora	H	1–9 Oct	90	969	0
Olaf	H	3–8 Oct	65	987	0
Patricia	H	20–26 Oct	70	984	0

^a T: Tropical storm, maximum sustained winds 34–63 kt; H: Hurricane, maximum sustained winds 64 kt or greater.

^b Dates based on UTC time and include tropical depression stage.

^c Reached maximum intensity in the central North Pacific hurricane basin.

teological analyses of all available observations. The best track consists of 6-hourly estimates of the center locations, maximum sustained (1-min average) surface (10 m) wind, and minimum sea level pressure. The life cycle of the cyclone (Table 1) includes the tropical (or subtropical) depression stage. However, it does not include the “remnant low” stage, the decay stage that commences when the organized convection dissipates, typically over colder water. Tracks of the 2003 tropical cyclones are shown in Fig. 2.

A vital (and often sole) source of information is imagery from geostationary meteorological satellites—the U.S. *GOES-10* and *-12*, which cover the eastern North Pacific basin. Tropical Cyclone intensity estimates can be obtained from the imagery using the Dvorak (1984) technique. Such estimates, or “classifications,” are provided every 6 h by the Tropical Analysis and Forecast Branch (TAFB) of the Tropical Prediction Center, the Satellite Analysis Branch of the National Environmental, Satellite, Data, and Information Service (NESDIS), and the Air Force Weather Agency. Geostationary satellites are also the source for wind vectors derived from the imagery through the methodology of Nieman et al. (1997).

GOES data are supplemented by data from low-earth-orbiting satellites. The most frequently used product is multichannel microwave imagery (Hawkins et al. 2001) from the Defense Meteorological Satellite Program polar-orbiting satellites and the National Aeronautics and Space Administration’s (NASA) Tropical Rainfall Measuring Mission. These data provide detailed information on TC convective structure and aid in determining center locations. Other products include information on thermal structure and intensity provided by the Advanced Microwave Sounding Unit on the National Oceanic and Atmospheric Administration’s polar-orbiting satellites (Brueske et al. 2002).

Other supplemental satellite information includes oceanic surface wind data from the NASA SeaWinds instrument on the Quick Scatterometer (QuikSCAT) and Advanced Earth Observing Satellite-2 satellites (Tsai et al. 2000). These data can help determine the extent of the TC wind field and help determine whether a tropical disturbance has a closed surface circulation.

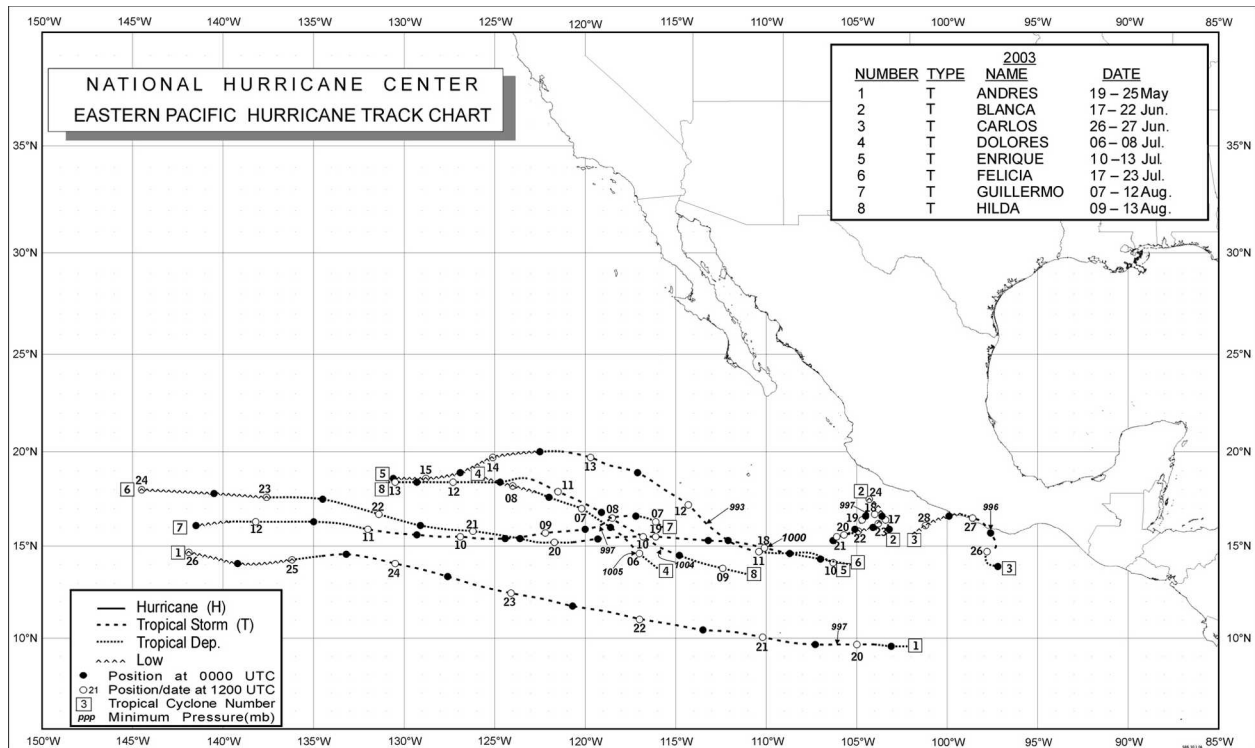
For systems posing a threat to land, in situ data are occasionally available from aircraft reconnaissance flights conducted by the Hurricane Hunters of the 53d Weather Reconnaissance Squadron of the Air Force Reserve Command. In the 2003 season, the Hurricane Hunters flew into Jimena while it passed south of Hawaii, and into Olaf off the coast of Mexico. During these flights, minimum central pressures are either measured by dropsondes released at the circulation center or extrapolated hydrostatically from flight-level temperature and pressure measurements. Surface or near-surface winds in the eyewall or maximum wind band are often measured directly using global positioning system (GPS) dropwindsondes (Hock and Franklin 1999), but are also frequently estimated from flight-level winds through empirical relationships derived from the GPS dropwindsondes (Franklin et al. 2000).

Other data sources include observations from ships, and from surface, upper-air, and radar stations in Mexico.

a. Tropical Storm Andres

While most eastern North Pacific TCs develop from Atlantic easterly waves (Avila et al. 2000), it is often difficult to track these disturbances, particularly early in the season. In the case of Andres, the initiating disturbance can be clearly tracked for only a few days prior to genesis. On 15 May, an area of disturbed weather developed south of Guatemala near 10°N lati-

(a)



(b)

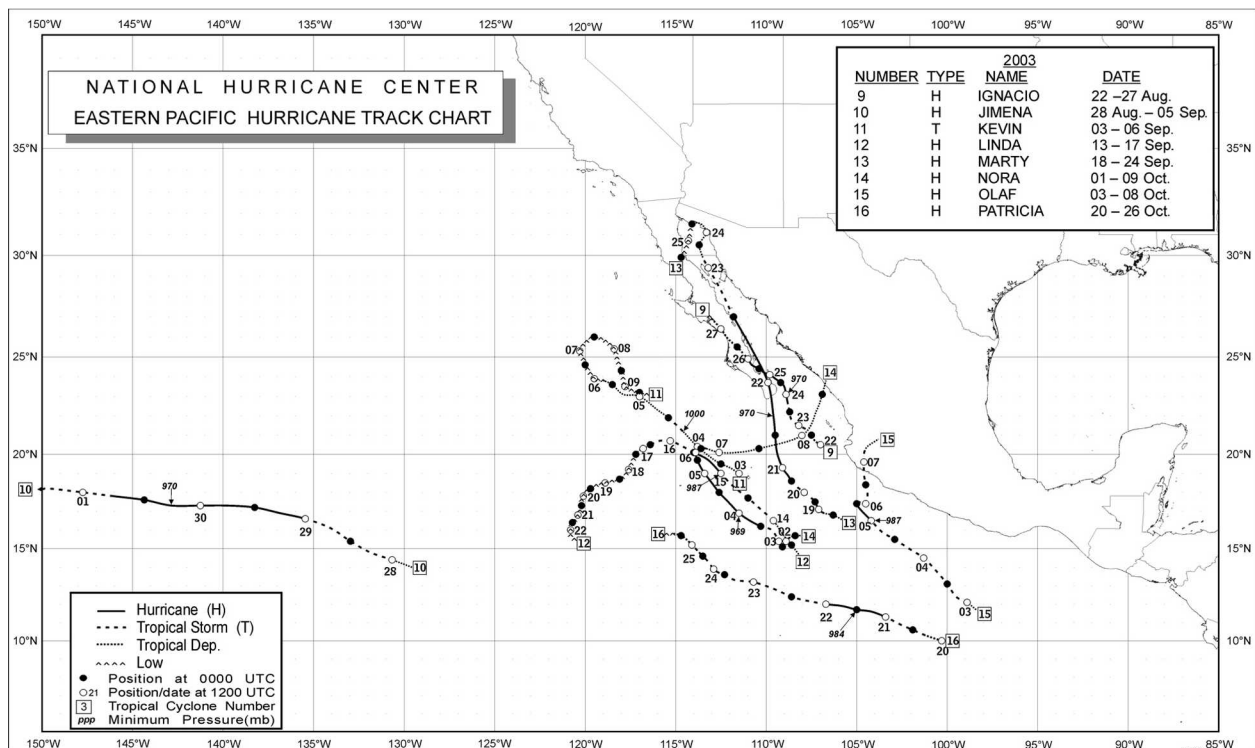


FIG. 2. Eastern North Pacific tropical storms and hurricanes of 2001: (a) numbers 1–8 and (b) numbers 9–16.

tude within a broad area of low pressure. This disturbance moved westward without development for the next three days. On 18 May, the convective pattern showed enough organization to warrant an initial Dvorak classification, and the system subsequently continued to develop. By 1800 UTC 19 May it had formed into a tropical depression about 920 n mi south-southeast of Cabo San Lucas, Mexico.

South of a large mid- to upper-level anticyclone, the depression moved westward and strengthened to a tropical storm by 0600 UTC 20 May. Later that day, the circulation center became exposed to the west of the main area of convection. Nevertheless, the convective banding became more pronounced, and scatterometer data suggest that Andres continued to strengthen, with maximum sustained winds reaching an estimated 50 kt by 1800 UTC.

Southwesterly shear stopped development, and for the next three days Andres maintained an estimated intensity of 45–50 kt. The midlevel anticyclone north of Andres shifted westward and helped steer Andres on a west-northwestward track at about 15–20 kt. During this period, the cyclone's low-level center remained near the western edge of intermittent convection that had a strong diurnal modulation. On 24 May, however, Andres crossed the 26°C sea surface temperature isotherm and the shear increased. Andres turned westward with the low-level flow and weakened to a tropical depression at 0600 UTC 25 May and degenerated to a nonconvective remnant low 6 h later. The remnant low dissipated about 1900 n mi west of Cabo San Lucas on 26 May.

b. Tropical Storm Blanca

A well-organized tropical wave, which crossed Central America on 12 June, moved westward and interacted with a preexisting area of disturbed weather. The shower activity became concentrated, and a tropical depression formed at 0000 UTC 17 June about 210 n mi south-southeast of Manzanillo, Mexico. The depression became a tropical storm by 1200 UTC that day. Blanca was embedded within a weak steering flow and first moved very slowly on a westward track, reaching estimated maximum sustained winds of 50 kt at 1800 UTC 18 June. Thereafter, Blanca drifted west-southwestward and began to weaken gradually because of strong southeasterly shear. It then began to meander while producing intermittent bursts of convection. It became a depression on 20 June and a remnant low on 22 June. The low drifted eastward for a day and a half and then moved west-northwestward until dissipation about 100 n mi south of Manzanillo by 1800 UTC on 24 June.

c. Tropical Storm Carlos

1) SYNOPTIC HISTORY

Carlos formed from a tropical wave that moved westward across the coast of Africa on 14 June. The wave

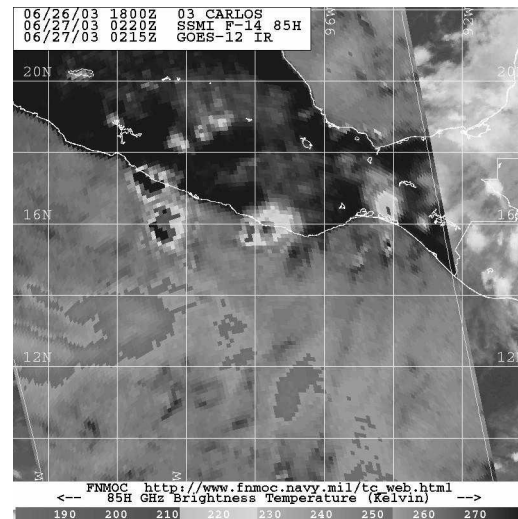


FIG. 3. Special Sensor Microwave Imager 85-GHz brightness image of Tropical Storm Carlos at 0200 UTC 27 Jun 2003. Image courtesy of the Naval Research Laboratory, Monterey, CA.

was almost indiscernible on satellite imagery during its 8-day crossing of the tropical Atlantic Ocean and Caribbean Sea. On 23 June, however, it developed into a concentrated area of disturbed weather south of the Gulf of Tehuantepec. As the disturbance drifted northward, the convection became better organized and a tropical depression formed early on 26 June about 120 n mi south of Puerto Escondido, Mexico.

Embedded in weak steering currents, the depression drifted erratically northward and strengthened, becoming a tropical storm at 1200 UTC on 26 June. Continuing slowly northward, Carlos strengthened to an estimated peak intensity of 55 kt before making landfall about 50 n mi west of Puerto Escondido early the next day.

Carlos quickly weakened below tropical storm intensity on 27 June as its circulation encountered the high terrain of Mexico. The depression began a slow westward drift that day, in response to weak steering from a deep-layer-mean ridge over Mexico. It then drifted westward to west-southwestward, moving back over the eastern Pacific waters for about 24 h and then dissipated early on 29 June.

2) METEOROLOGICAL STATISTICS

The landfall intensity estimate of 55 kt was based primarily on the appearance of an eyelike feature on microwave imagery just before landfall (Fig. 3) and also on the appearance of a similar feature on radar images from the Puerto Angel radar.

Three ships reported tropical-storm force winds associated with Carlos. The *Sealand Champion* reported 40-kt winds at 1800 UTC 26 June, while the *Raicho II* reported 37-kt winds and a 1001.0-mb pressure 3 h later. A ship with the call sign NEPP reported 35-kt

winds at 0000 UTC 27 June. There were no observations of tropical-storm-force winds from land stations.

3) CASUALTY AND DAMAGE STATISTICS

No deaths were reported. According to the Associated Press, there were no reports of serious damage. However, more than 40 coastal communities in the Mexican state of Oaxaca sustained some flooding, along with downed power lines and phone service.

d. Tropical Storm Dolores

Radiosonde data from the Windward Islands indicate that a tropical wave entered the eastern Caribbean Sea on 27 June. It is difficult, however, to trace this wave back to Africa. The system moved westward and entered the eastern North Pacific basin on 30 June. An area of disturbed weather associated with the wave received its initial Dvorak classification on 3 July at 1800 UTC while centered about 625 n mi south of Manzanillo. Deep convection associated with the disturbance fluctuated for a couple of days, but became more persistent on 5 July. The disturbance became a tropical depression around 0600 UTC 6 July about 655 n mi south-southwest of Cabo San Lucas. Slight strengthening occurred, and the depression became a tropical storm 6 h later. At that time, maximum sustained winds were estimated at their peak of 35 kt. East-northeasterly shearing then adversely affected Dolores, and later on 6 July, the low-cloud center became exposed to the northeast of the main area of convection.

A midlevel ridge north and northeast of Dolores caused the cyclone to move west-northwestward to northwestward throughout the short life cycle. This motion soon took Dolores over lower (below 25°C) sea surface temperatures. Aside from a few brief bursts, deep convection associated with the cyclone generally diminished after the system reached tropical storm strength. Dolores weakened back to a tropical depression around 0000 UTC 8 July and diminished to a remnant low located about 800 n mi west-southwest of Cabo San Lucas 6 h later. The low dissipated by 0000 UTC 9 July.

e. Tropical Storm Enrique

Enrique formed from a tropical wave that departed the coast of Africa on 25 June. The wave moved quickly westward with minimal shower activity until it reached northern South America and the western Caribbean Sea on 4 July. The wave emerged over the eastern North Pacific Ocean on 6 July accompanied by a surface low pressure system. Thunderstorm activity became organized enough for satellite classifications to begin on 9 July. Subsequent satellite intensity estimates indicated that a tropical depression formed at 1200 UTC 10 July about 565 n mi south-southeast of Cabo San Lucas. The depression gradually became better or-

ganized, and it is estimated that it became a tropical storm at 1200 UTC 11 July. Enrique moved west-northwestward for the next 2 days and it is estimated that it reached its peak intensity of 55 kt early on 12 July.

The genesis of Enrique occurred relatively close to the cooler sea surface temperatures that normally exist off the west coast of Baja California. Late on 12 July, Enrique encountered those cooler waters and began to weaken despite the otherwise favorable low vertical wind shear across the tropical storm. Rapid weakening began early on 13 July, and Enrique became a tropical depression at 1200 UTC. The cyclone then turned westward and degenerated into a nonconvective low pressure system by 0000 UTC 14 July. The low continued moving westward over colder water until it dissipated early on 16 July about 1200 n mi west-southwest of Cabo San Lucas.

f. Tropical Storm Felicia

Felicia formed from a tropical wave that moved westward across the coast of Africa on 4 July. The wave crossed Central America on 12 July and passed south of the Gulf of Tehuantepec on 14 July. At that time, convection began to increase in coverage and organization, and the first satellite intensity estimates were made the next day. Convection further increased in organization on 17 July, and it is estimated that a tropical depression formed about 315 n mi south of Manzanillo near 1800 UTC that day. The depression became a tropical storm early on 18 July and reached an estimated peak intensity of 45 kt later that day. After that, vertical wind shear caused gradual weakening, with Felicia becoming a depression again on 20 July. During that period, the cyclone moved generally westward, followed by a west-northwestward turn on 21 July. Felicia continued to slowly weaken, and it degenerated to a remnant low on 23 July. The low crossed into the central Pacific hurricane basin (140°W to the international date line) later that day and dissipated on 24 July about 600 n mi east of Hawaii.

g. Tropical Storm Guillermo

Guillermo developed from a tropical wave that moved into the Atlantic from the African coast on 22 July and crossed into the eastern North Pacific on 1 August. On 4 August, when the wave axis was south of Baja California, the wave amplitude and the associated convective activity increased noticeably, and the system received its first Dvorak classification. Surface analyses indicate the development of a weak surface low on 6 August. By late on 6 August, convection associated with the low became isolated from the larger-scale wave, and the surface circulation associated with the low became better defined. It is estimated that a tropical depression formed at 0600 UTC 7 August, about 525 n mi southwest of Cabo San Lucas.

Guillermo formed to the south of a low- to midlevel ridge that built westward and strengthened over the following few days, and this kept the tropical cyclone on a basically westward track. Under light southerly shear initially, the depression became better organized and reached tropical storm strength by 0000 UTC 8 August. The estimated maximum sustained winds of 50 kt were reached at 1800 UTC 8 August and maintained for nearly 24 h. However, Guillermo was soon affected by the upper-level outflow from developing Tropical Storm Hilda about 600 n mi to the east. The convection became disrupted and the cyclone began to weaken on 9 August. Guillermo weakened to a tropical depression on 11 August. The shear then shifted to westerly and Guillermo's convection diminished on 12 August, when the depression degenerated to a remnant low about 1750 n mi west of Cabo San Lucas. The remnant low moved into the central Pacific basin before dissipating the next day.

h. Tropical Storm Hilda

Hilda developed from a tropical wave that left the coast of Africa on 27 July and moved westward across the tropical Atlantic and the Caribbean Sea accompanied by intermittent convection. The wave first showed persistent thunderstorm activity on 5 August when it was in the eastern North Pacific a few hundred miles south of the Gulf of Tehuantepec. The system moved westward while the convection gradually increased in organization, and it became a tropical depression about 600 n mi south of Cabo San Lucas. Upper-level outflow was fairly impressive over the western semicircle, but the outflow was inhibited elsewhere by strong easterly shear. This allowed only limited intensification to occur. The cyclone reached its estimated maximum intensity of 35 kt at 0600 UTC 10 August. Thereafter, Hilda moved on a general west-northwestward track and encountered cooler waters and westerly shear. As a weakening cyclone, Hilda moved westward, steered by the low-level flow, and dissipated by 1800 UTC 13 August about 1200 n mi west-southwest of Cabo San Lucas.

i. Hurricane Ignacio

1) SYNOPTIC HISTORY

Ignacio is believed to have originated from a tropical wave that moved from Africa to the tropical Atlantic Ocean on 6 August. The wave moved westward without distinction, crossing Central America and entering the Pacific Ocean on 16 August. Cloudiness associated with the wave gradually increased and became organized into a distinct area of disturbed weather by 20 August just south of Manzanillo. Two days later, the disturbed weather became well enough organized to be classified as a tropical depression about 190 n mi southeast of Cabo San Lucas.

A midlevel subtropical ridge lay north of Ignacio

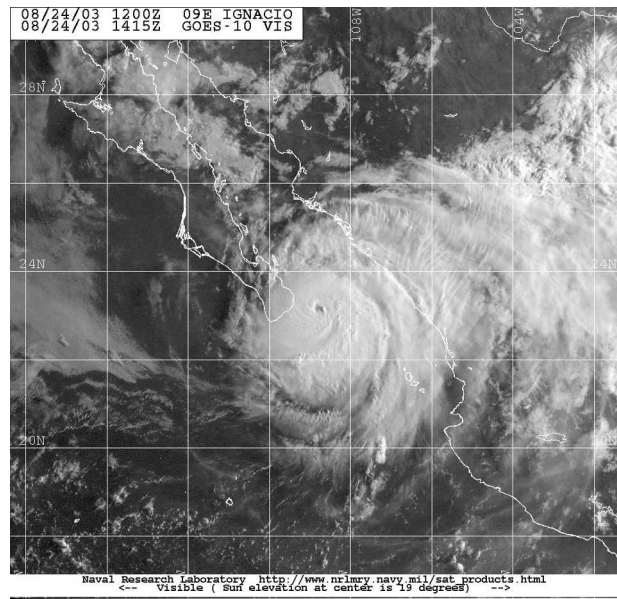


FIG. 4. GOES-10 visible image of Hurricane Ignacio at 1415 UTC 24 Aug 2003. Image courtesy of the Naval Research Laboratory, Monterey, CA.

throughout its lifetime. However, Ignacio was embedded in a weakness within the ridge and this resulted in a slow, mostly northwestward motion.

The depression quickly strengthened to a tropical storm early on 23 August and into the first eastern North Pacific hurricane of 2003 early on 24 August. Ignacio reached an estimated peak intensity of 90 kt (SSHS category 2) later that day, when the center came within 25 n mi of the southeastern tip of Baja California (Fig. 4). The hurricane made landfall on 25 August just east of La Paz, Mexico, with winds having decreased to an estimated 70 kt by that time. This weakening likely resulted from interaction with high terrain, and it continued while Ignacio moved over Baja California. Ignacio weakened to a tropical depression on 26 August and dissipated late on 27 August over central Baja California.

2) METEOROLOGICAL STATISTICS

There were no reliable reports of tropical-storm-force or greater wind associated with Ignacio.

3) CASUALTY AND DAMAGE STATISTICS

Hurricane-force winds blew down trees, signs, and power lines in La Paz and elsewhere in southern Baja California, but the strongest winds bypassed Cabo San Lucas. Rainfall totals were large because of Ignacio's slow movement, and serious inland floods resulted. Two rescue workers were swept to their deaths by freshwater floods.

j. Hurricane Jimena

Jimena may have originated from a tropical wave that crossed Central America and entered the eastern North Pacific in mid-August. This system was difficult to track as it moved westward, however, and it is uncertain if the wave was related to an area of disturbed weather within the intertropical convergence zone near 125°W on 26 August from which Jimena developed. The disturbed weather drifted westward and became better organized, resulting in the system being classified by the Dvorak technique at 1800 UTC 27 August. It is estimated that a tropical depression formed near 0600 UTC 28 August about 1500 n mi east of the Hawaiian Islands.

The depression quickly became a tropical storm, then strengthened further in an environment of weak vertical shear and warm ocean waters. A small eye developed, and Jimena attained hurricane status around 1200 UTC 29 August. With a deep-layer ridge to its north, the hurricane moved on a generally west-northwestward track. This was followed by a westward turn as a slight weakness in the ridge northwest of the hurricane gradually filled in. This brought Jimena into the central Pacific basin shortly after 0600 UTC 30 August. Strengthening continued, and the cyclone's estimated maximum sustained winds reached 90 kt around 1800 UTC 30 August (Fig. 5). Thereafter, Jimena gradually weakened, and its winds fell below hurricane strength on 1 September. Moving westward to west-southwestward, the center of the weakening storm passed about 105 n mi south of the southern tip of the island of Hawaii at 1500 UTC 1 September. Jimena moved westward to west-southwestward and continued weakening because of increased vertical shear and possibly because of a more stable environmental air mass. It weakened to a tropical depression by 0000 UTC 3 September and maintained winds of 25 to 30 kt for a few more days as it moved generally westward. Jimena crossed the international date line on 5 September and dissipated shortly afterward, about 1500 n mi west-southwest of the Hawaiian Islands.

Jimena brought tropical-storm-force gusts to portions of the Hawaiian Islands. The island of Kahoolawe reported a gust of 50 kt, while South Point on the island of Hawaii reported a gust of 46 kt. Rainfall of 152 to 254 mm and high surf were reported on the island of Hawaii in association with Jimena. Neither casualties nor significant damage were reported.

k. Tropical Storm Kevin

Kevin originated from a tropical wave that moved across the west coast of Africa on 20 August. The wave was largely devoid of thunderstorm activity until reaching the eastern North Pacific Ocean late on 28 August. A broad surface low pressure area developed along the wave axis by 29 August, although the associated convection remained poorly organized. For the next 2 days,

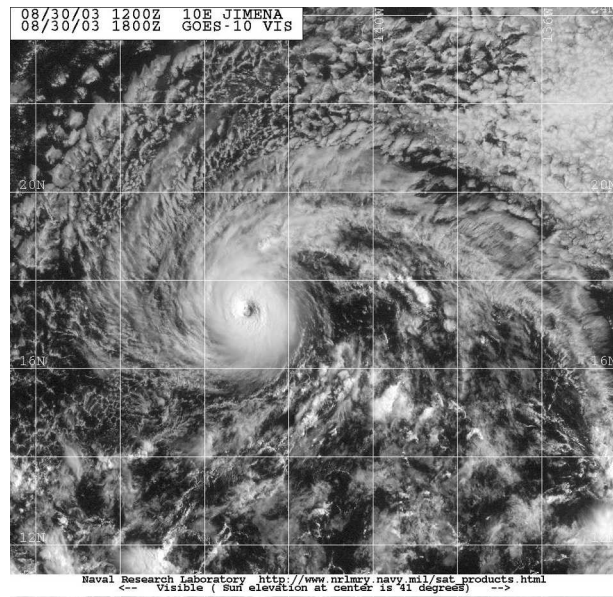


FIG. 5. GOES-10 visible image of Hurricane Jimena at 1800 UTC 30 Aug 2003. Image courtesy of the Naval Research Laboratory, Monterey, CA.

the unusually large low moved west-northwestward around the western periphery of a subtropical ridge located across central Mexico and the eastern North Pacific. Surface pressures continued to fall despite the lack of organized central convection. Sufficient persistent convection formed near the center for Dvorak classification to begin early on 3 September. By 1200 UTC that day, the disturbance became a tropical depression about 245 n mi south-southwest of Cabo San Lucas.

Like Enrique, Kevin developed close to unfavorably cool sea surface temperatures. This, combined with the broad circulation, likely prevented rapid development. It is estimated that the depression briefly became a tropical storm at 1800 UTC 4 September while moving west-northwestward. Although upper-level winds appeared favorable for strengthening, Kevin weakened back to a tropical depression 6 h later while moving over cooler water. Kevin continued moving west-northwestward and gradually degenerated into a non-convective low pressure system by 1200 UTC 6 September. The remnant low was slow to dissipate. It meandered and looped slowly for the next 4 days before dissipating on 10 September about 365 n mi west of Cabo San Lucas.

l. Hurricane Linda

Linda formed from a tropical wave that emerged from the coast of Africa on 28 August. The system moved westward with little development, crossing Central America and entering into the Pacific on 6 September. Convection began to increase on 9 September and became better organized on 12 September as a broad

surface low formed. Development continued, and it is estimated that the disturbance became a tropical depression near 1800 UTC 13 September, about 340 n mi southwest of Manzanillo.

The depression moved northwestward and intensified. It became a tropical storm on 14 September and a hurricane with estimated 65-kt winds the next day. Linda was a hurricane for only 12 h before it weakened to a tropical storm early on 16 September. The storm turned westward later that day, followed by a southwestward turn on 17 September while it weakened to a depression. Linda became a remnant low on 18 September about 445 n mi west-southwest of Cabo San Lucas, and the low drifted southwestward and south-southwestward until dissipation on 23 September.

m. Hurricane Marty

1) SYNOPTIC HISTORY

Marty developed from a tropical wave that moved into the eastern North Pacific basin on 10 September. Convection associated with the wave became more persistent on 16 September south of Manzanillo, and on 18 September the convection began to organize. The system received its initial Dvorak classification at 1200 UTC that day, and it is estimated that a tropical depression formed by 1800 UTC, about 450 miles south-southeast of Cabo San Lucas.

South of a weak midlevel ridge and in a light shear environment, the depression moved slowly toward the west-northwest and strengthened, becoming a tropical storm at 0600 UTC 19 September. Development slowed during the following 24 h, perhaps due to relatively dry air entraining into the system from the east. Around 1200 UTC 20 September, the very intense but previously shapeless convection organized into bands and the pace of development increased while the system moved slowly northwestward. Marty became a hurricane at 0000 UTC 21 September. Late on 21 September, Marty turned north-northwestward around the periphery of the midlevel ridge and began to accelerate and strengthen in a region of enhanced upper-level divergence. By 0600 UTC 22 September the estimated maximum sustained winds reached their peak of 85 kt (SSHS category 2). Marty was moving northward at about 17 kt when it made landfall at 0930 UTC 22 September near San Jose del Cabo, Mexico, just east of Cabo San Lucas, with winds near 85 kt (Fig. 6).

A few hours later, Marty again turned north-northwestward, and the center entered the Gulf of California near La Paz. The hurricane moved along the eastern coast of southern Baja California south of Santa Rosalia, Mexico, during the remainder of 22 September. Marty weakened to a tropical storm by 0000 UTC 23 September near Santa Rosalia, and then headed into the northern Gulf of California where it was stalled by a midlevel high over Nevada. Although winds decreased, Marty continued to produce heavy rains that

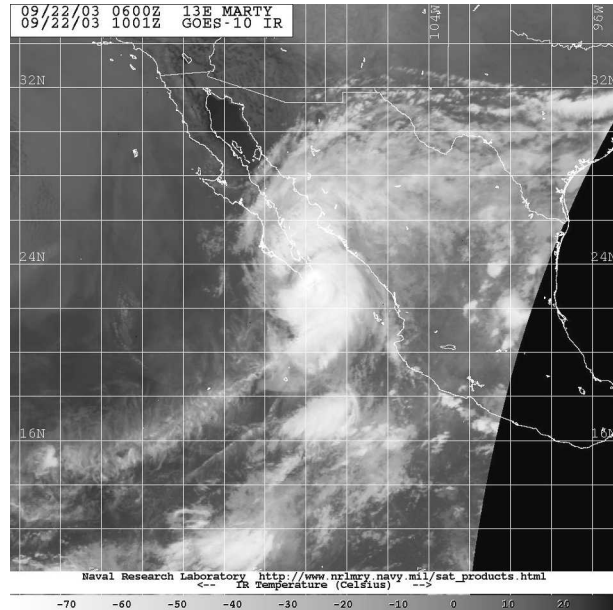


FIG. 6. GOES-10 infrared image of Hurricane Marty at 1001 UTC 22 Sep 2003. Image courtesy of the Naval Research Laboratory, Monterey, CA.

first affected northwestern mainland Mexico and then spread into Arizona, New Mexico, and western Texas. Deep convection associated with the cyclone began to diminish, and Marty weakened to a tropical depression late on 23 September. Over the next 2 days Marty meandered in and around the northern Gulf of California, degenerating to a nonconvective remnant low by 0000 UTC 25 September. The remnant circulation drifted south-southwestward and dissipated over the northern Baja California peninsula early on 26 September.

2) METEOROLOGICAL STATISTICS

Marty brought hurricane conditions to portions of the southern Baja California peninsula, with tropical storm conditions reported in a number of locations farther north, including Santa Rosalia on the Baja peninsula and Los Mochis on the Mexican mainland (Table 2). An automated station at Cabo San Lucas recorded 10-min mean winds of 76 kt with a gust to 102 kt. Cabo San Lucas also reported 203.2 mm of rain.

Two ships encountered Marty on 19 September. The *Zim Iberia* reported 35-kt winds at 0600 UTC 19 September; this was an important observation in upgrading Marty to a tropical storm. The *Leverkusen Express* reported 35-kt winds at 2100 UTC that same day. The SV *Sea Witch*, anchored in La Paz harbor, reported a pressure of 971.9 mb on 22 September as the center of Marty passed over (Table 2).

3) CASUALTY AND DAMAGE STATISTICS

The government of Mexico reported 12 direct deaths associated with Marty in three states: 5 in Baja Califor-

TABLE 2. Selected surface observations for Hurricane Marty, 18–24 Sep 2003.

Location	Minimum sea level pressure		Maximum surface wind speed			Total rain (mm)
	Date/time (UTC)	Pressure (mb)	Date/time (UTC) ^a	Sustained (kt) ^c	Gust (kt)	
Mexico						
Cabo San Lucas			22/0900	76	102	203.2
Loreto	22/2100	983.8 ^b				150.6
Santa Rosalia	22/2300	1003.1 ^b	23/0000	33	53	197.1
La Paz						119.4
La Paz Harbor SV <i>Sea Witch</i>		971.9				
Todos Santos						197.6
Los Mochis	22/1600	1002.0 ^b	22/1600	40 ^b		
Arizona						
Organ Pipe Cactus National Monument						57.2
Tanque Verde						46.2
Red Mountain						43.9
Tucson International Airport						43.2
Three Points						42.2
Corona de Tucson						40.9

^a Date/time is for sustained wind when both sustained and gust are listed.

^b Record incomplete. More extreme values may have occurred.

^c 10-min average.

nia del Sur, 5 in Sonora, and 2 in Sinaloa. These totals include two individuals officially listed as missing but presumed dead. Media reports indicate that the deaths in Baja California del Sur were associated with vehicles being swept away by rising river waters, with some or all of the deaths in Sonora associated with the sinking of a fishing boat near Guaymas. Monetary damages are unknown, although media reports indicate that roughly 4000 homes were damaged in southern Baja California. There was extensive damage to marine interests in the La Paz area, in Puerto Escondido, and in other locations along the Baja peninsula. Some beach erosion was reported at San Felipe in the northern Gulf of California.

n. Hurricane Nora

Nora developed from a tropical wave that left the coast of Africa on 13 September. This wave nearly developed into a tropical depression on several occasions as it moved westward across the Atlantic and the Caribbean Sea. The wave crossed Central America on 25 September accompanied by numerous thunderstorms. The convective activity continued westward near the southern coast of Mexico for several days. However, it was not until 1800 UTC 1 October that the system became organized into a tropical depression about 525 n mi south of Cabo San Lucas. Strengthening occurred, and the system became a tropical storm at 0600 UTC 2 October. Nora moved slowly westward and then west-northwestward and reached hurricane status at 0000 UTC 4 October. The hurricane reached its estimated peak intensity of 90 kt 12 h later. Nora maintained hurricane status for 2 days as it continued moving slowly northwestward. The cyclone then turned to the east and northeast ahead of a strong middle-level

trough. This trough, and the outflow from Hurricane Olaf to the southeast, produced strong southwesterly shear that resulted in Nora's weakening. Nora weakened to a tropical storm at 1200 UTC 6 October and to a tropical depression at 0600 UTC 7 October. The poorly defined center of Nora reached the coast of Mexico just north of Mazatlan early on 9 October and rapidly dissipated over high terrain.

According to reports from the Meteorological Service of Mexico, the impact of Nora was minimal, and there were no reports of damages or casualties. Heavy rains, however, did affect the state of Sinaloa.

o. Hurricane Olaf

Olaf formed from a tropical wave that moved from Africa to the Atlantic Ocean on 17 September and moved westward to the eastern Pacific during the following two weeks. The wave was difficult to track for several days in the Atlantic Ocean and eastern Caribbean Sea. The system first showed signs of organization on 2 October when centered about 400 n mi south-southeast of Acapulco, Mexico. Microwave and visible satellite imagery showed increased organization on 3 October, and it is estimated that a tropical depression formed near 0600 UTC that day about 325 n mi south-southeast of Acapulco.

The depression strengthened to a tropical storm with 50-kt winds in 12 h as it moved northwestward around the southwestern periphery of a weak midlevel anticyclone over Mexico. Olaf continued this motion for 2 days while reaching an estimated peak intensity of 65 kt at 1200 UTC 5 October. A radar at Cuyutlan, Mexico, showed a partial eyewall at this time. Soon after, the cloud structure became disorganized, and Olaf is estimated to have been a hurricane for only a few hours.

TABLE 3. Official and CLIPER track forecast errors in the eastern North Pacific basin for the 2003 season and for the period 1993–2002, including depression phases.

	Forecast period (h)						
	24	36	48	72	96	120	
2003 average official error (n mi)	36	64	91	116	173	248	340
2003 average CLIPER error (n mi)	42	84	133	182	275	401	533
2003 average official error relative to CLIPER	–14%	–23%	–31%	–36%	–37%	–38%	–36%
2003 No. of cases	258	228	198	169	118	73	36
1993–2002 average official error (n mi)	39	72	103	131	185		
1993–2002 No. of cases	2864	2595	2316	2054	1605		
2003 official error relative to 1993–2002 official	–8%	–10%	–11%	–11%	–7%		

Gradually weakening and slowing in forward speed, the storm moved or reformed toward the east early on 6 October. It then resumed a slow northward track and moved inland just west of Manzanillo on 7 October, with estimated sustained winds of 50 kt. The slow forward motion allowed for considerable rainfall over southwestern Mexico. Olaf dissipated over the high terrain of Mexico by early on 8 October.

Although tropical cyclones Nora and Olaf were roughly 650 n mi apart, there was little apparent interaction between the two cyclones, save for the impact of the outflow of Olaf on the intensity of Nora.

1) METEOROLOGICAL STATISTICS

The Air Force Reserve Hurricane Hunters made one flight into Olaf. The maximum flight-level winds were 64 kt at a flight level of 850 mb at 2038 UTC on 5 October. The standard reduction of 80% converts a 64-kt wind at 850 mb to a surface wind speed of 51 kt. The lowest central pressure measured by the aircraft was 992 mb at about the same time as the maximum flight-level winds.

There were no observations of tropical-storm force winds from land stations. A ship with the call sign ABCA2 reported 47-kt winds at 1800 UTC 3 October.

2) CASUALTY AND DAMAGE STATISTICS

A document from ReliefWeb titled “Mexico: Post-hurricane flooding appeal No. 22/03” (ReliefWeb 2003) indicates that there were no reported deaths. However, rain-induced floods caused severe damage to homes, crops, and roads in the states of Jalisco and Guanaajuato. More than 12 000 houses in Jalisco were damaged by the floods.

p. Hurricane Patricia

A distinct tropical wave crossed Central America on 17 October and moved over the eastern North Pacific Ocean on 18 October. As the wave moved westward to the south of Mexico over the following couple of days, the associated deep convection consolidated and organized into curved bands. The system received its first Dvorak classification at 2345 UTC 19 October. Devel-

opment continued, and it is estimated that a tropical depression formed by 1200 UTC 20 October, centered about 400 n mi south of Acapulco. The depression strengthened into a tropical storm 6 h later. Around 1200 UTC 21 October, an eye was apparent on satellite imagery, suggesting that Patricia had become a hurricane. The hurricane reached its estimated peak intensity of 70 kt about 12 h later. Patricia was embedded in an east-southeasterly steering current to the south of a deep-tropospheric ridge. This caused the cyclone to move west-northwestward at 8 to 12 kt for a few days, roughly parallel to, and well offshore of, the coast of Mexico.

On 22 October, an upper-level trough near the Baja California peninsula created increasing westerly vertical shear over Patricia, displacing the main area of deep convection east of the low-level center. The system weakened below hurricane strength by 1200 UTC that day. Patricia continued to weaken until around 1200 UTC 24 October, when the shear apparently relaxed a bit, and the center became embedded within the deep convection again. This resulted in slight restrengthening. Later on 24 October, Patricia turned toward the northwest in response to a weakness in the ridge caused by the trough near Baja California. A final weakening trend began about the same time. Patricia weakened to a depression by 1200 UTC 25 October, and by 0600 UTC 26 October it had weakened to a remnant low about 520 n mi south-southwest of Cabo San Lucas. The low turned westward in response to the near-surface flow, and soon became indistinct.

3. Forecast verification

Every 6 h, the National Hurricane Center issues an advisory “package” for all TCs in the eastern North Pacific basin. This package includes 12-, 24-, 36-, 48-, 72-, (and for the first time in 2003) 96-, and 120-h official forecasts of the TC center location and maximum 1-min wind speed (at 10-m elevation) associated with the cyclone circulation. These forecasts are verified by comparison with the best-track positions and wind speeds. A track forecast error is defined as the great-circle distance between a forecast center location and a

TABLE 4. Official and SHIFOR intensity forecast errors in the eastern North Pacific basin for the 2003 season and for the period 1993–2002, including depression phases.

	Forecast period (h)						
	12	24	36	48	72	96	120
2003 average official error (kt)	6.1	10.7	14.9	18.5	20.7	18.6	20.1
2003 average SHIFOR error (kt)	6.7	10.7	15.2	19.5	23.3	21.4	21.3
2003 average official error relative to SHIFOR	−9%	0%	−2%	−5%	−11%	−13%	−6%
2003 No. of cases	256	227	198	168	118	73	36
1993–2002 average official error (kt)	6.1	10.9	14.6	17.0	20.1		
1993–2002 No. of cases	2851	2574	2305	2044	1605		
2003 official error relative to 1993–2002 official	0%	−2%	2%	9%	3%		

best-track position for the same time. A wind speed forecast error is the absolute value of the difference between a forecast wind speed and best-track wind speed. One change introduced to the forecast verification in 2003 is that 96- and 120-h forecasts are included, as well as forecasts from the tropical depression phase. This was not the case in previous annual summaries.

Table 3 lists the official average track forecast errors for the 2003 season and the average error for the 10-yr period 1993–2002. Also listed are the Climatology–Persistence (CLIPER) model track errors for 2003. The CLIPER model is a simple statistical model derived from the best tracks of past TCs (Aberson 1998); it represents a “no skill” accuracy level.

The 2003 average official track forecast errors are 7% to 11% smaller than those of the past 10 yr for the 12, 24, 36, 48, and 72 h. The track forecast errors are smaller than the corresponding CLIPER errors—14% smaller at 12 h, 23% smaller at 24 h, and 31% to 38% smaller at other times. This shows that the track forecasts had skill relative to that measure. Track errors for the CLIPER model in 2003 (not shown) were larger than those for the 10-yr average, and thus the 2003 forecasts had a higher amount of skill relative to that measure than the previous 10 yr.

Table 4 lists the official average wind speed forecast errors for the 2003 season and for the 10-yr period 1993–2002. SHIFOR model intensity errors are also listed. The Statistical Hurricane Intensity Forecast model (SHIFOR) (Jarvinen and Neumann 1979) is a statistical wind speed forecast model and is the analog to CLIPER for determining the skill of a wind speed forecast.

The 2003 official wind speed errors equaled or were higher than the 10-yr average at all times save 24 h. The forecast errors were also similar to those of SHIFOR, as improvements over that method ranged to only 13% at 96 h to no improvement at 24 h. Intensity errors for SHIFOR in 2003 (not shown) were less than those for the 10-yr average all times save 72 h, where they were about equal. Thus, the 2003 forecasts had less skill relative to that measure than in the previous 10 yr.

Acknowledgments. The authors wish to thank the Naval Research Laboratory’s tropical cyclone Web page team headed by Jeff Hawkins and the NASA GOES Project at the Goddard Space Flight Center for the satellite imagery. Stephen R. Baig produced the track charts. The Meteorological Service of Mexico provided the meteorological data for that country.

REFERENCES

- Aberson, S. D., 1998: Five-day tropical cyclone track forecasts in the North Atlantic basin. *Wea. Forecasting*, **13**, 1005–1015.
- Avila, L. A., R. J. Pasch, and J. Jiing, 2000: Atlantic tropical systems of 1996 and 1997: Years of contrasts. *Mon. Wea. Rev.*, **128**, 3695–3706.
- Brueske, K. F., C. S. Velden, B. W. Kabat, and J. D. Hawkins, 2002: Tropical cyclone intensity estimation using the NOAA-KLM Advanced Microwave Sounding Unit (AMSU): Part 1—Initial field test and lessons learned. Preprints, *25th Conf. on Hurricanes and Tropical Meteorology*, San Diego, CA, Amer. Meteor. Soc., 481–482.
- Dvorak, V. F., 1984: Tropical cyclone intensity analysis using satellite data. NOAA Tech. Rep. NESDIS 11, 47 pp.
- Franklin, J. L., M. L. Black, and K. Valde, 2000: Eyewall wind profiles in hurricanes determined by GPS dropwindsondes. Preprints, *24th Conf. on Hurricanes and Tropical Meteorology*, Fort Lauderdale, FL, Amer. Meteor. Soc., 446–447.
- Hawkins, J. D., T. F. Lee, J. Turk, C. Sampson, F. J. Kent, and K. Richardson, 2001: Real-time Internet distribution of satellite products for tropical cyclone reconnaissance. *Bull. Amer. Meteor. Soc.*, **82**, 567–578.
- Hock, T. F., and J. L. Franklin, 1999: The NCAR GPS dropwindsonde. *Bull. Amer. Meteor. Soc.*, **80**, 407–420.
- Jarvinen, B. R., and C. J. Neumann, 1979: Statistical forecasts of tropical cyclone intensity for the North Atlantic basin. NOAA Tech. Memo. NWS NHC-10, 22 pp.
- Nieman, S. J., W. P. Menzel, C. M. Hayden, D. Gray, S. T. Wanzong, C. S. Velden, and J. Daniels, 1997: Fully automated cloud-drift winds in NESDIS operations. *Bull. Amer. Meteor. Soc.*, **78**, 1121–1133.
- ReliefWeb, 2003: Mexico: Post-hurricane flooding Appeal No. 22/03. [Available online at <http://www.reliefweb.int/w/rwb.nsf>.]
- Simpson, R. H., 1974: The hurricane disaster potential scale. *Weatherwise*, **27**, 169, 186.
- Tsai, W.-Y., M. Spender, C. Wu, C. Winn, and K. Kellogg, 2000: SeaWinds of QuikSCAT: Sensor description and mission overview. *Proc. Geoscience and Remote Sensing Symp. 2000*, Vol. 3, Honolulu, HI, IEEE, 1021–1023.